The background of the slide is a scenic landscape. It features a wide river or lake in the foreground, reflecting the sky. The middle ground is filled with dense green trees and foliage. The sky is a mix of soft pinks, oranges, and blues, suggesting a sunset or sunrise. The overall mood is serene and natural.

THE ORIGIN OF THE SLOW SOLAR WIND

Leon Ofman

Department of Physics

The Catholic University of America and
NASA Goddard Space Flight Center

Introduction

- Observations by **Ulysses** (McComas et al 1998, 2000), **UVCS** (Raymond et al 1997; 1998; Habbal et al 1997; Strachan et al 2002), **LASCO** (Sheeley et al 1997, 1999; Tappin et al 1999; Lewis & Simnett 2000, 2002), and **Doppler Scintillation** (Woo & Gazis 1994) associate the slow solar wind with dense equatorial regions – streamer belts.
- Correlation between physical properties of the slow/fast solar wind and the ion composition has been found with Ulysses and ACE (e.g., Geiss 1995; Wimmer-Schweingruber et al 1997; Zurbuchen et al 2000, 2002; Pagel et al 2004).
- Pneuman and Kopp (1971) attempted the first 2D MHD steady state model of a self-consistent solar wind flow in a coronal streamer, and since then the coronal streamers were extensively

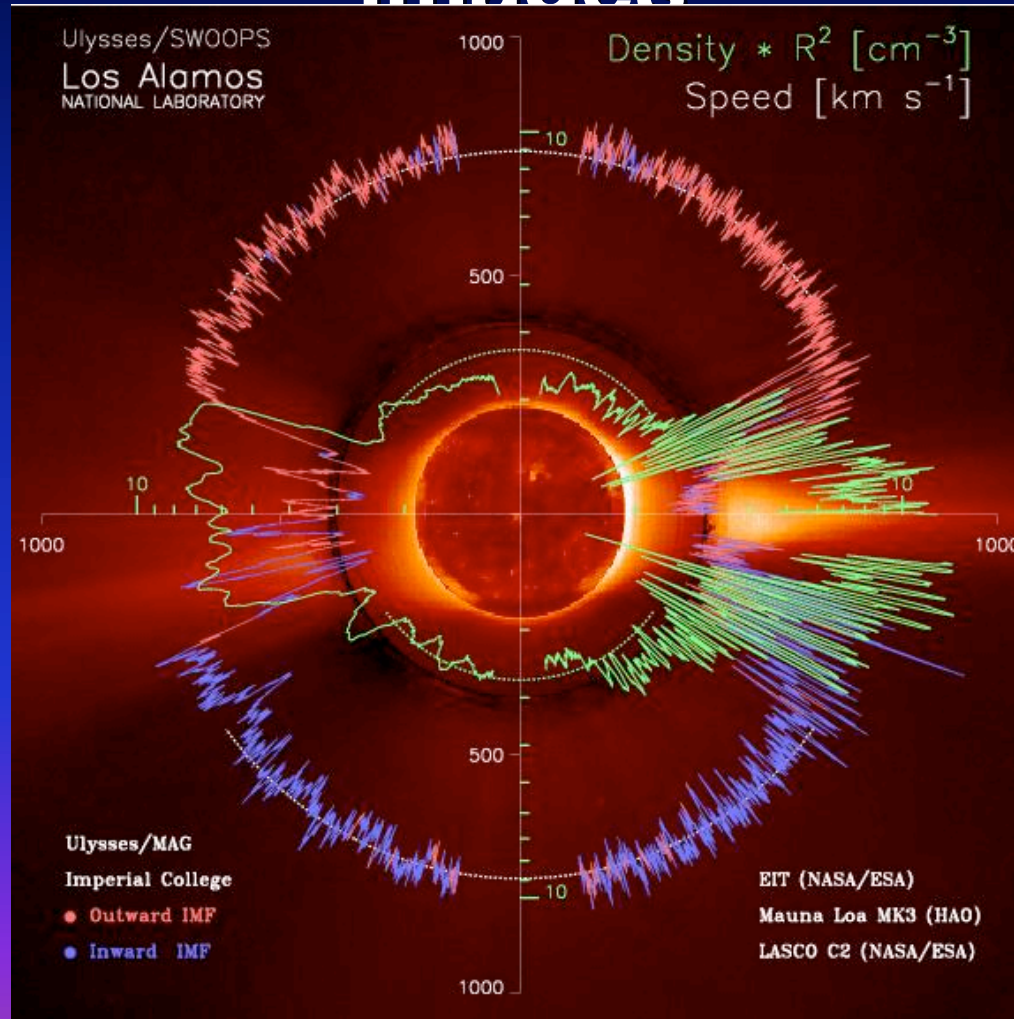
Introduction

- **2D MHD** models (Steinolfson et al 1982; Washimi et al 1987; Cuperman et al 1990, 1995; Usmanov 1993, 2000; Wu et al 1995; Wang et al 1993, 1998; Suess et al 1994, 1996; Bravo and Stewart 1997; Wiegelmann et al 2000; Li et al 2001; Endeve et al 2003).
- Empirical heating **2D MHD** models (Sittler & Guhathakurta 1999; Sittler et al 2002, 2003).
- As part of **3D MHD** global models (Linker et al 1990, 1999; Usmanov 1992, 1993; Usmanov and Goldstein 2003; Pizo 1994, 1995; Mikic & Linker 1995; Mikic et al 1999).
- **Two-fluid** models (Suess et al 1999; Endeve et al 2004).
- **Three-fluid** models (Ofman 2000, 2004).
- Magnetized wake of a streamer was considered by Dahlburg et al (1997); Karpen and Dahlburg (1998), and Einaudi et al (1999, 2001) as a source of the slow wind.
- Fisk (1999) proposed open-emerging closed field reconnection model for the origin of the solar wind.

Slow solar wind (SSW) – main unresolved issues

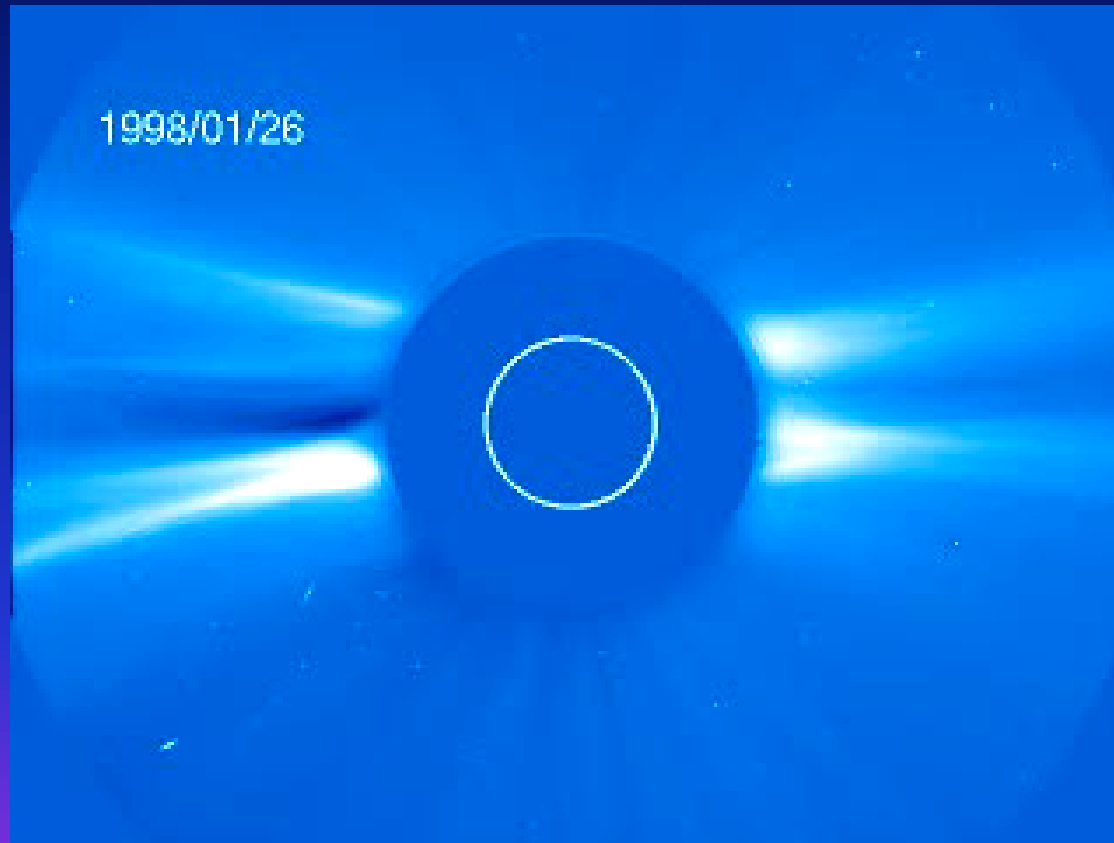
- What heats the SSW plasma?
- What determines the composition of the SSW?
- What are the physical mechanisms that produce the “unsteady” SSW?
- How the streamer magnetic field, density, temperature, composition and flow structure affects the SSW?
- What are the stability properties of streamers?

Overlay of Ulysses/SWOOPS speed, density and EIT/LASCO/Mauna Loa images



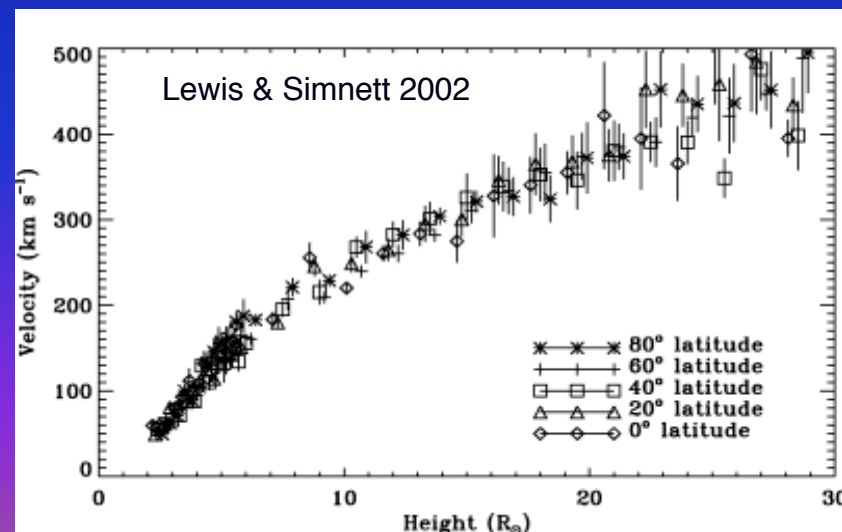
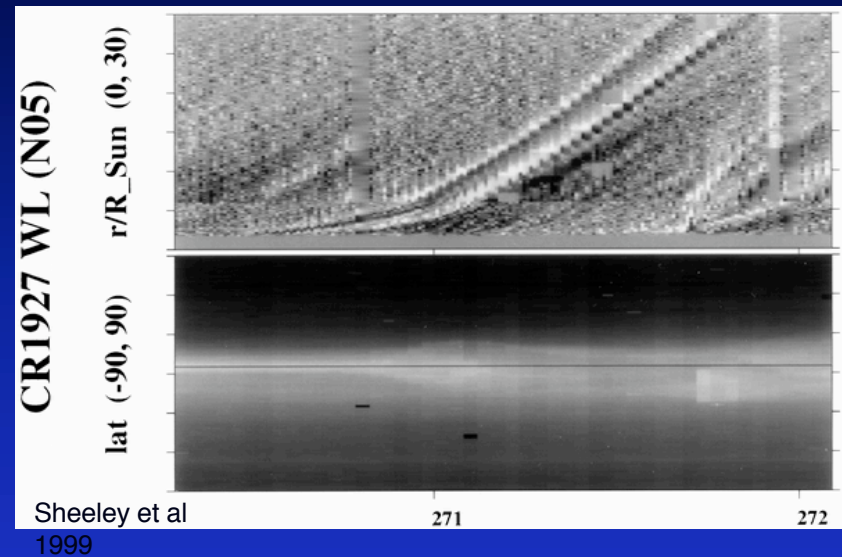
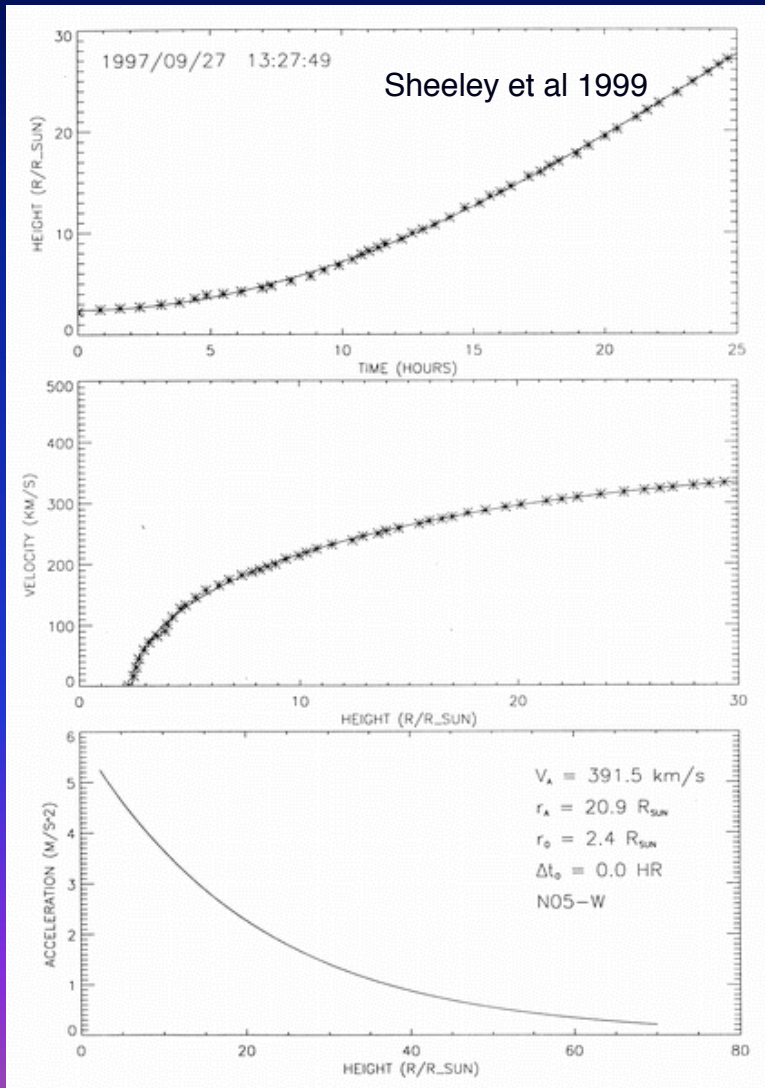
McComas et al., JGR, 105, 10419,
2000

LASCO/C2 Observations

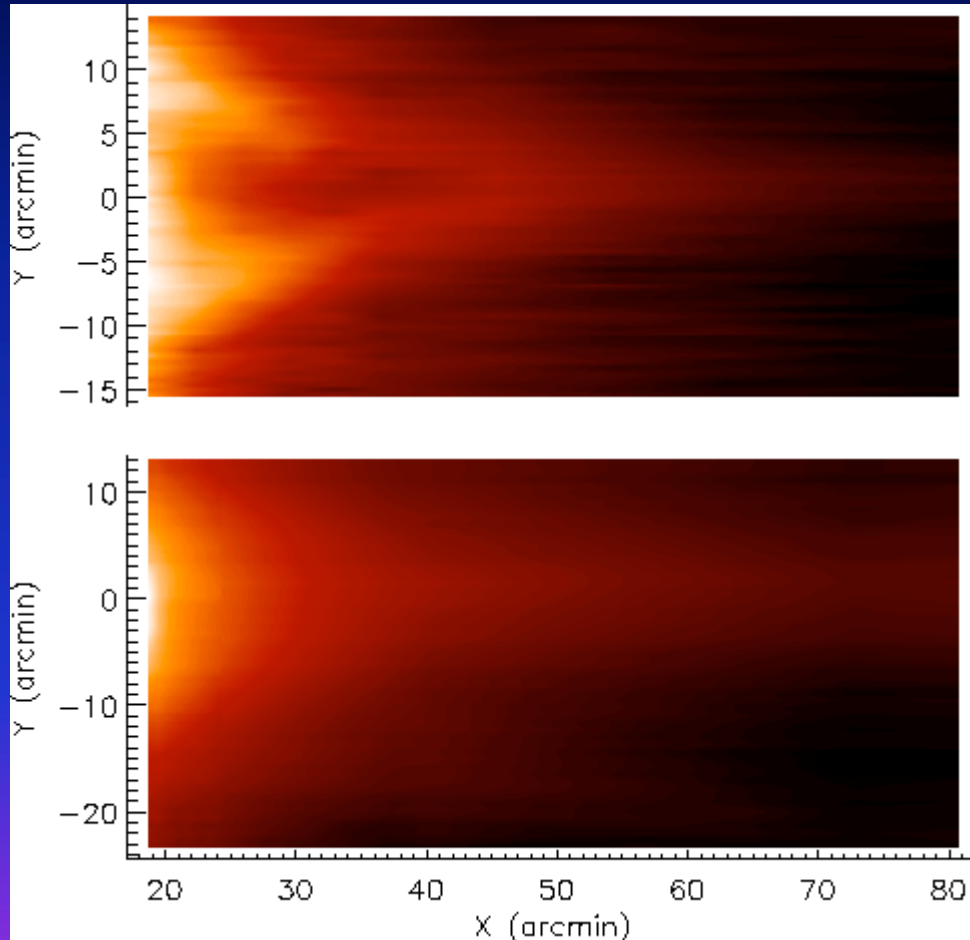


Continuous C2 observations from Jan 26, 1998 to Feb 26, 1998

LASCO Observations



UVCS EUV Observations

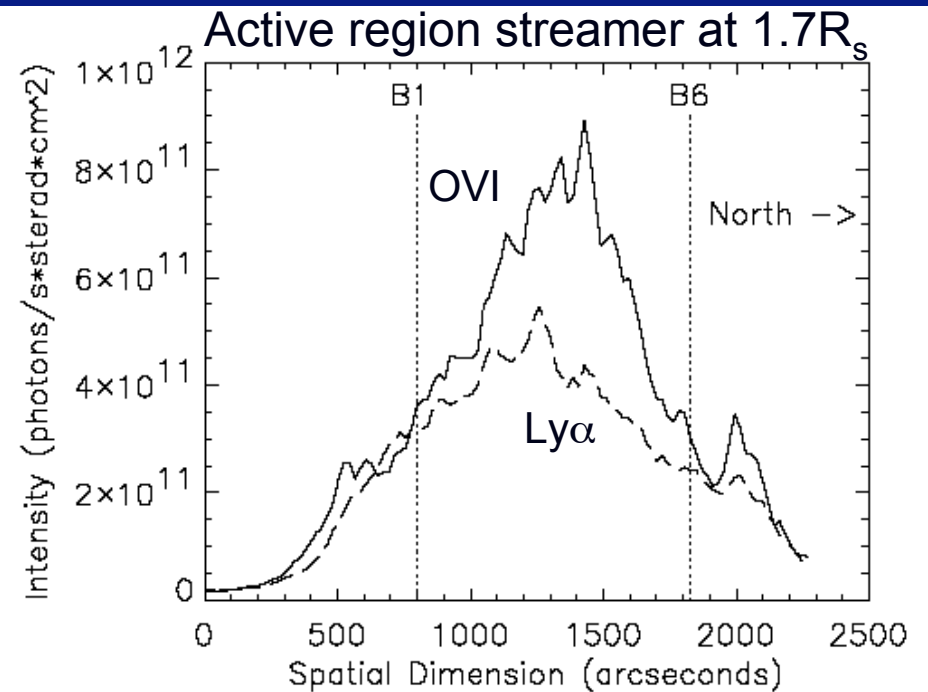
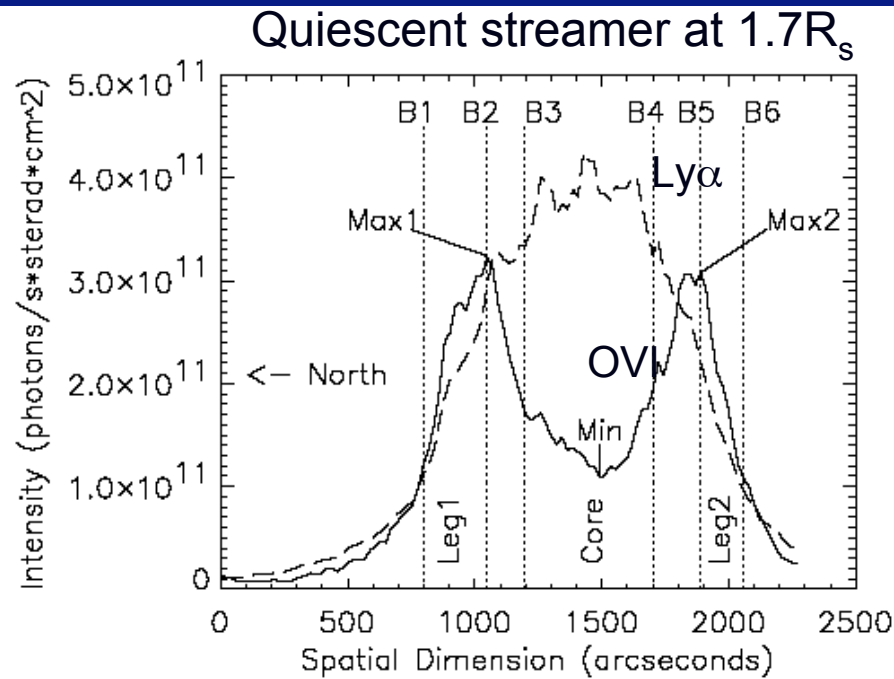


Equatorial streamer above the west limb of the Sun on October 12, 1996. The upper panel shows the streamer in the light of O 5+ ions at 103.2 nm. The lower panel shows the same streamer in the light from neutral hydrogen atoms (H I) at 121.6 nm (Lyman α). The Y axis gives solar coordinates in arc min, originating in the center of the disk, where positive Y axis is the projected heliographic north direction. The X axis is approximately in the heliographic west direction.

(Kohl et al 1997)

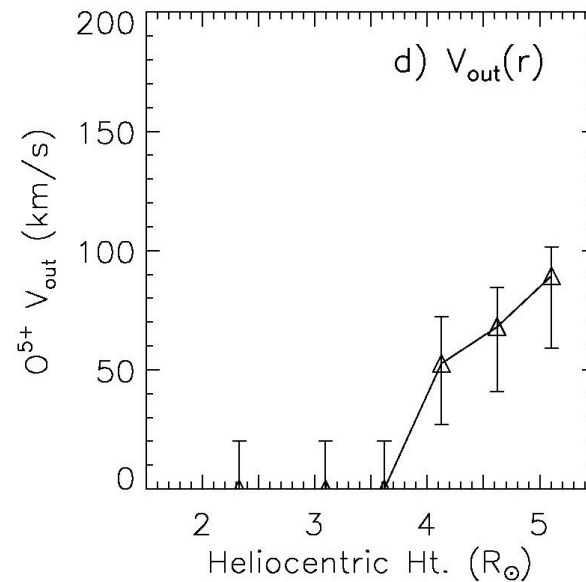
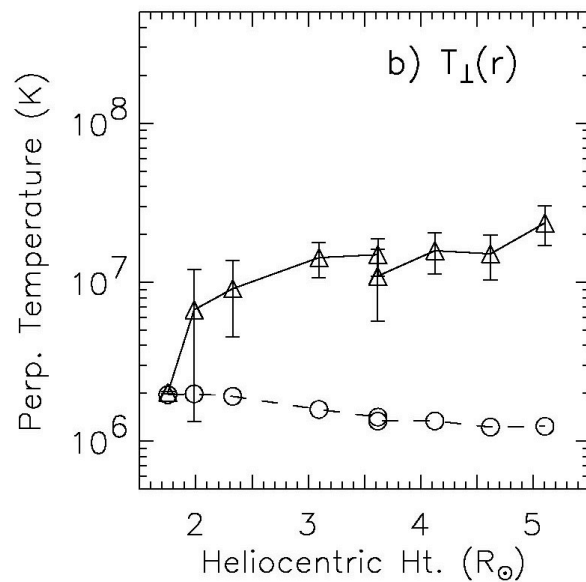
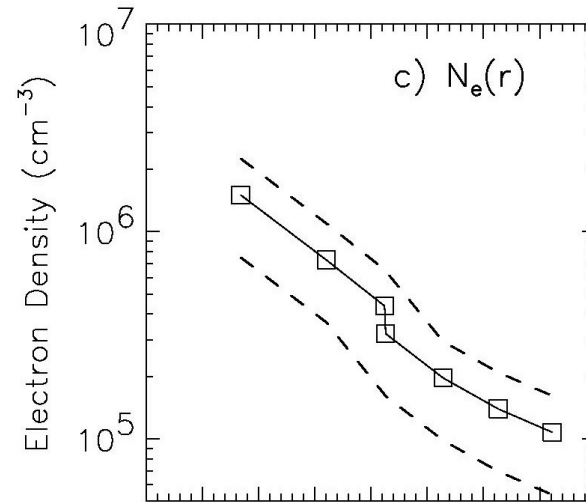
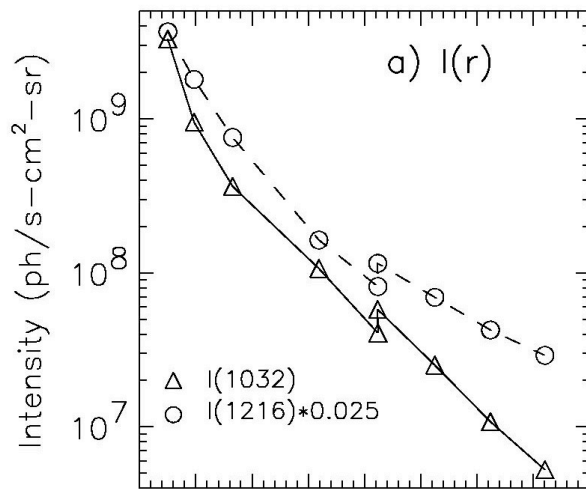
Streamer Composition

SOHO/UVCS



Uzzo et al (2003)
Similar results for Si XII and Mg X

UVCS Observations (Strachan et al 2002)



Three-fluid equations

Normalized three fluid equations for $V \ll c$, with gravity, resistivity, viscosity, and Coulomb friction, neglecting electron inertia, assuming quasi-neutrality:

$$\frac{\partial n_k}{\partial t} + \nabla \cdot (n_k \mathbf{V}_k) = 0,$$

$$n_k \left[\frac{\partial \mathbf{V}_k}{\partial t} + (\mathbf{V}_k \cdot \nabla) \mathbf{V}_k \right] = -E_{uk} \nabla p_k - E_{ue} \frac{Z_k n_k}{A_k n_e} \nabla p_e - \frac{n_k}{F_r r^2} \mathbf{e}_r \\ + \frac{Z_k e}{A_k m_p c} n_k (\mathbf{V}_k - \mathbf{V}_e) \times \mathbf{B} + \mathbf{F}_v + n_k \mathbf{F}_{k,coul},$$

$$\frac{\partial \mathbf{B}}{\partial t} = -\nabla \times \mathbf{E}, \quad \mathbf{E} = -\mathbf{V}_e \times \mathbf{B} + \frac{1}{S} \nabla \times \mathbf{B}$$

$$\mathbf{V}_e = \frac{1}{n_e} (n_p \mathbf{V}_p + Z_i n_i \mathbf{V}_i - b \nabla \times \mathbf{B}),$$

$$\frac{\partial T_k}{\partial t} = -(\gamma_k - 1) T_k \nabla \cdot \mathbf{V}_k - \mathbf{V}_k \cdot \nabla T_k + C_{kjl} + (\gamma_k - 1) (H_k + S_k),$$

where Z_k is the charge number; A_k is the atomic mass number of species k .

$$\beta_k = 5/3$$

Heating and loss terms

- Empirical heating term with $S_0=2$, $\lambda_k=0.7R_s$
- Heat conduction term for electrons and protons along field lines.
- Radiative losses
- Ohmic and viscous heating can be

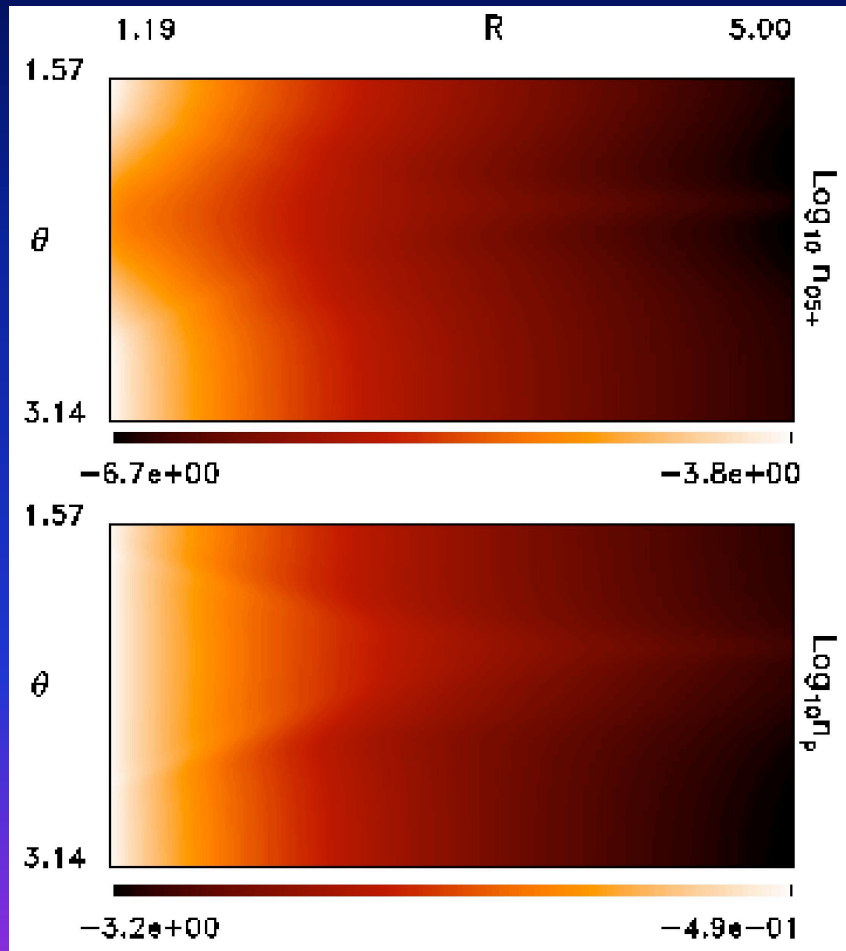
$$S_k = S_{0,k} (1 - r) e^{r/\lambda_k}$$

$$H_k = \lambda_k^{-1} \mathbf{B} \cdot \left[\lambda_k T_k^{2.5} \frac{T_k \cdot \mathbf{B}}{B^2} \right]$$

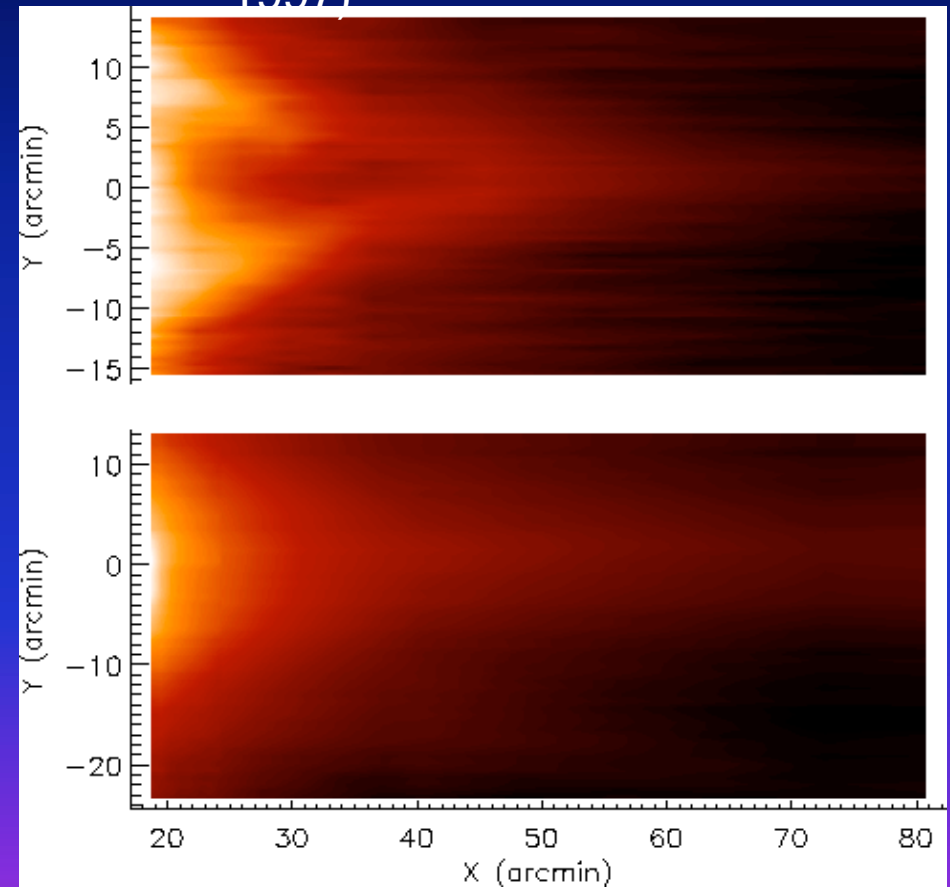
$$S_r = n_e^2 (T_e)$$

Three-fluid model vs. UVCS observations

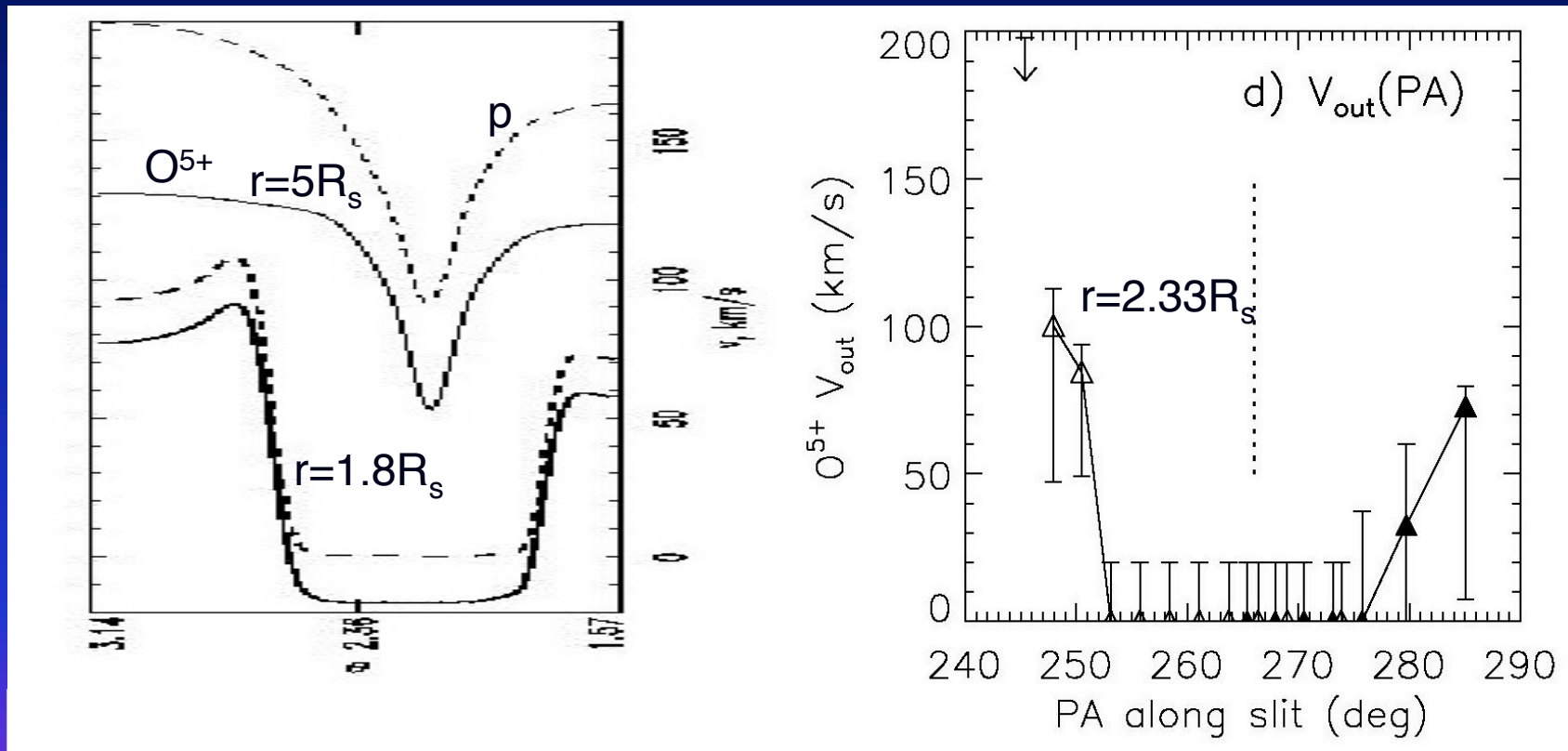
3-fluid model (Ofman 2000)



UVCS Observations (Kohl 1997)

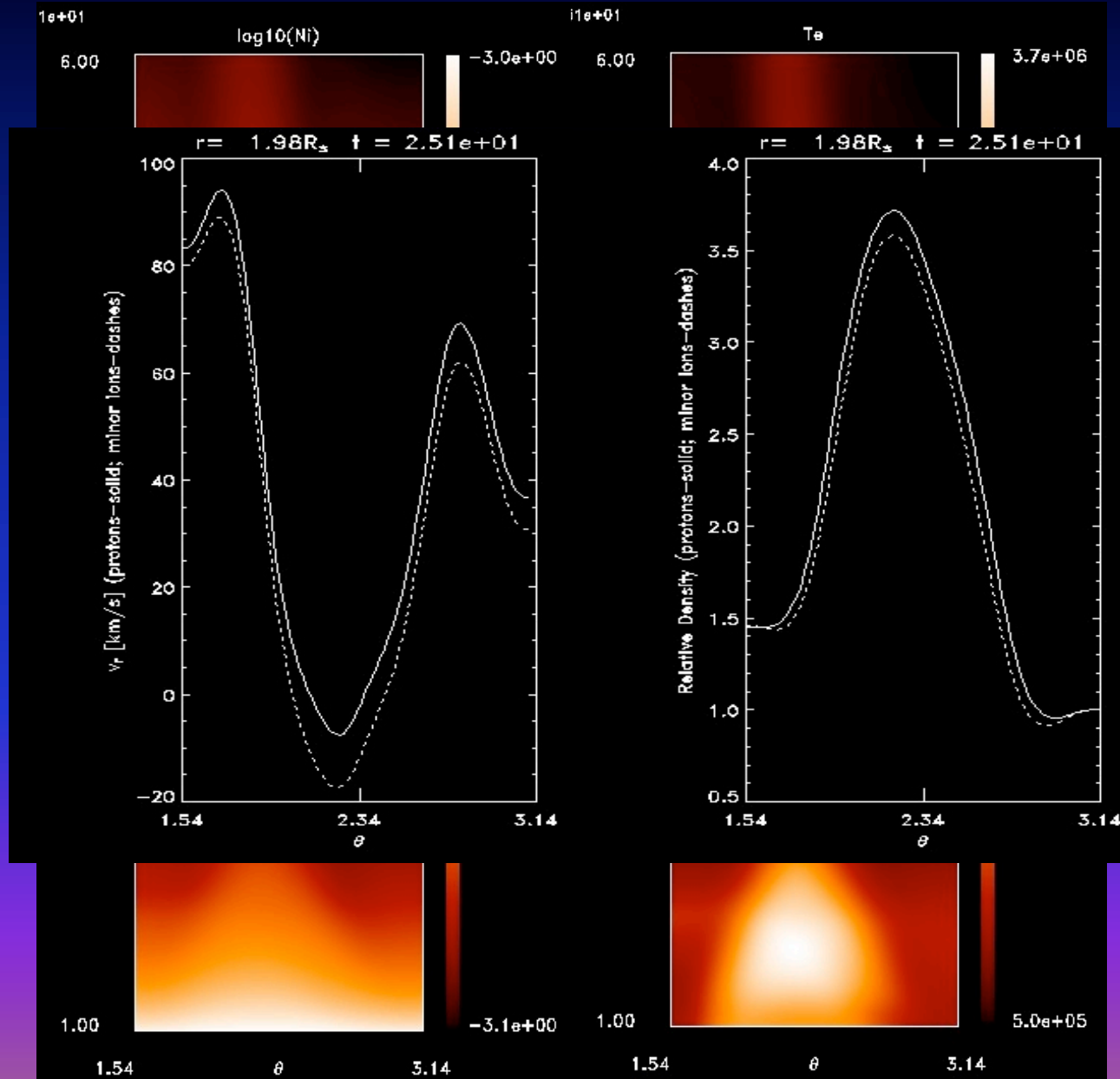


Three-fluid model vs. UVCS observations

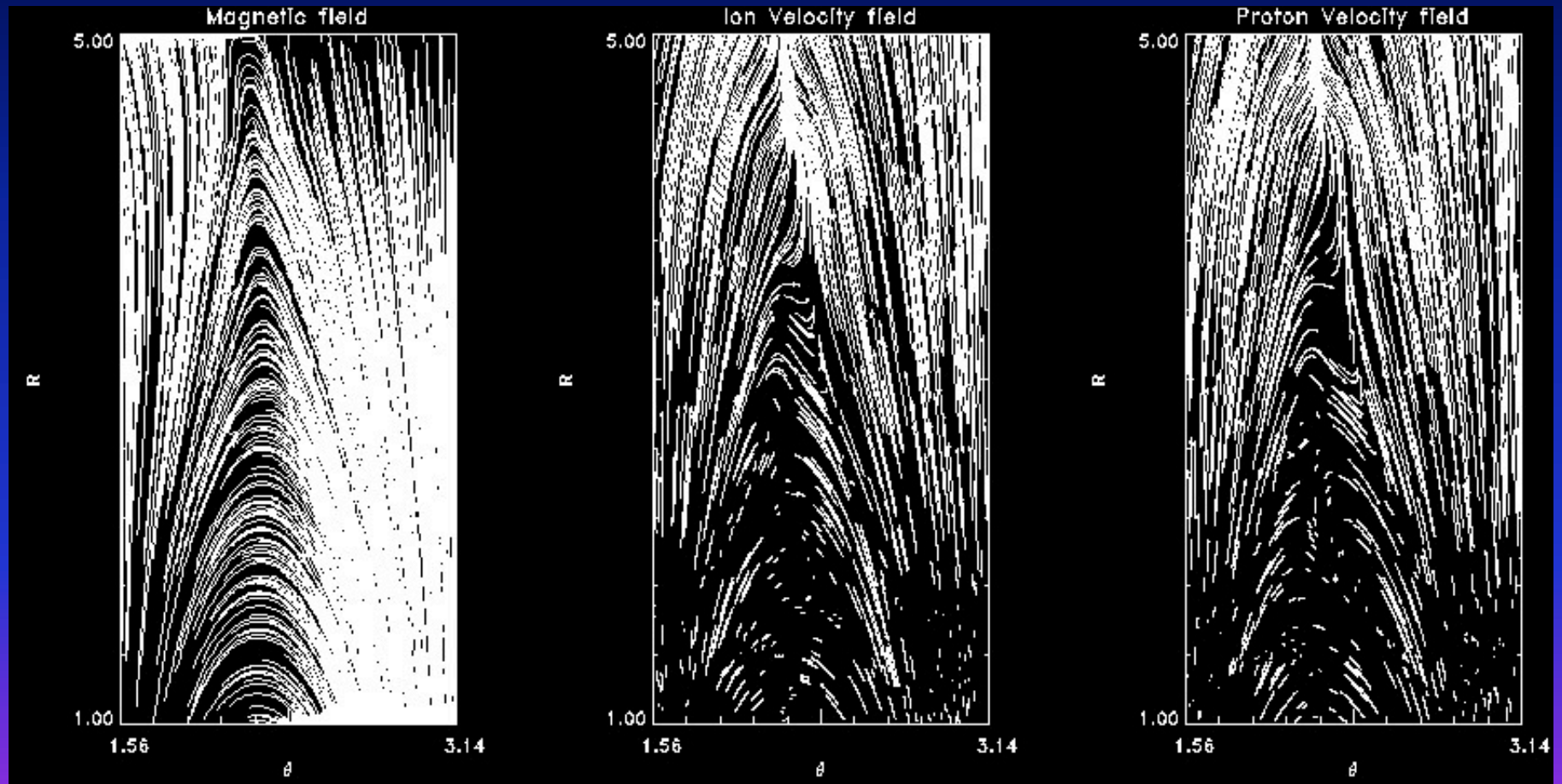


(Strachan et al 2002)

“Active region” streamer model



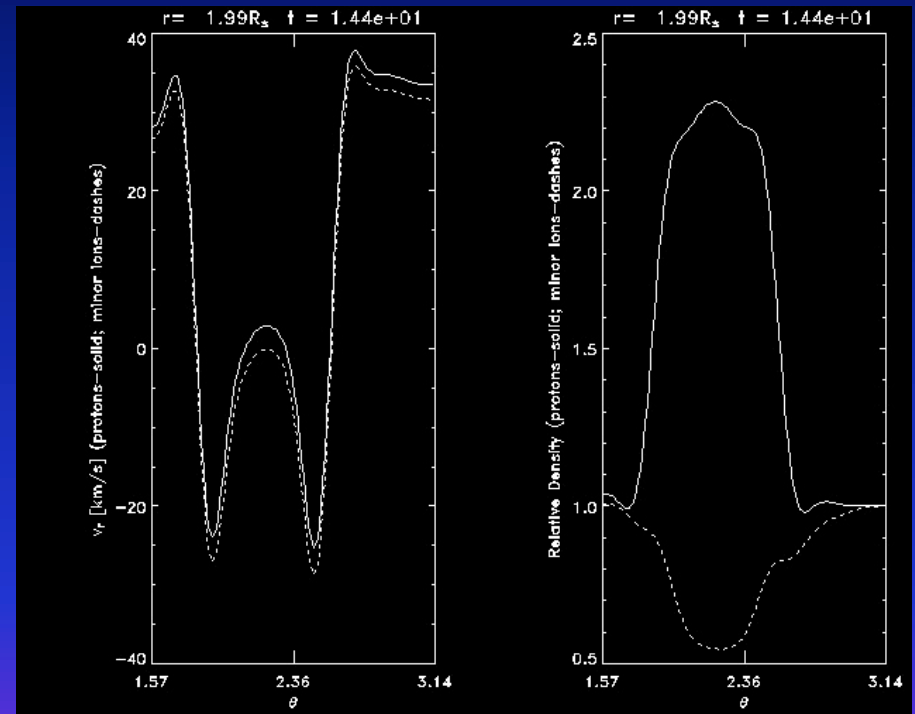
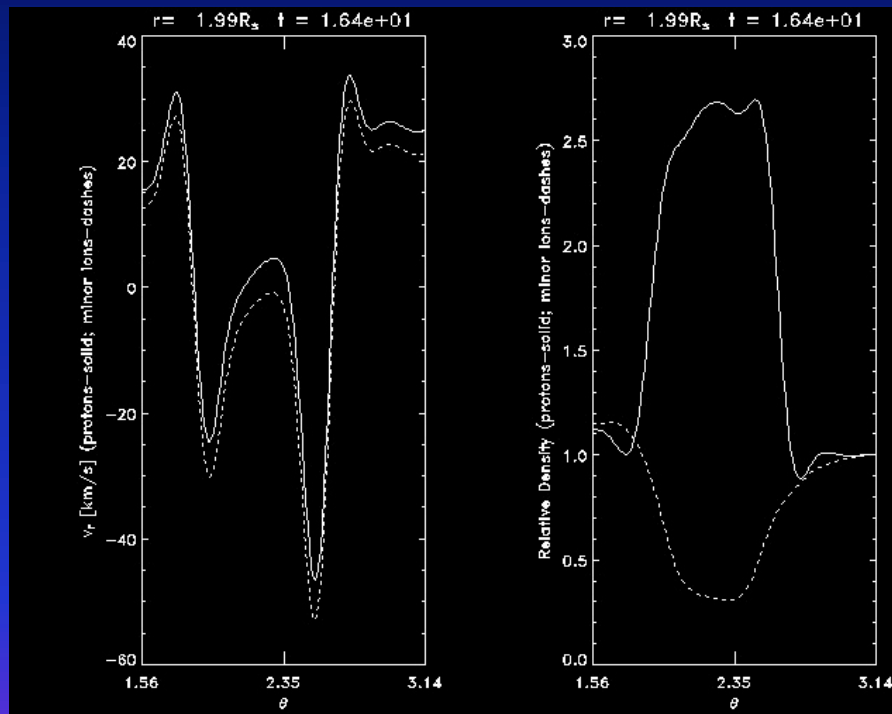
Magnetic field and flow



O⁵⁺ vs He⁺⁺

O⁵⁺

He⁺⁺

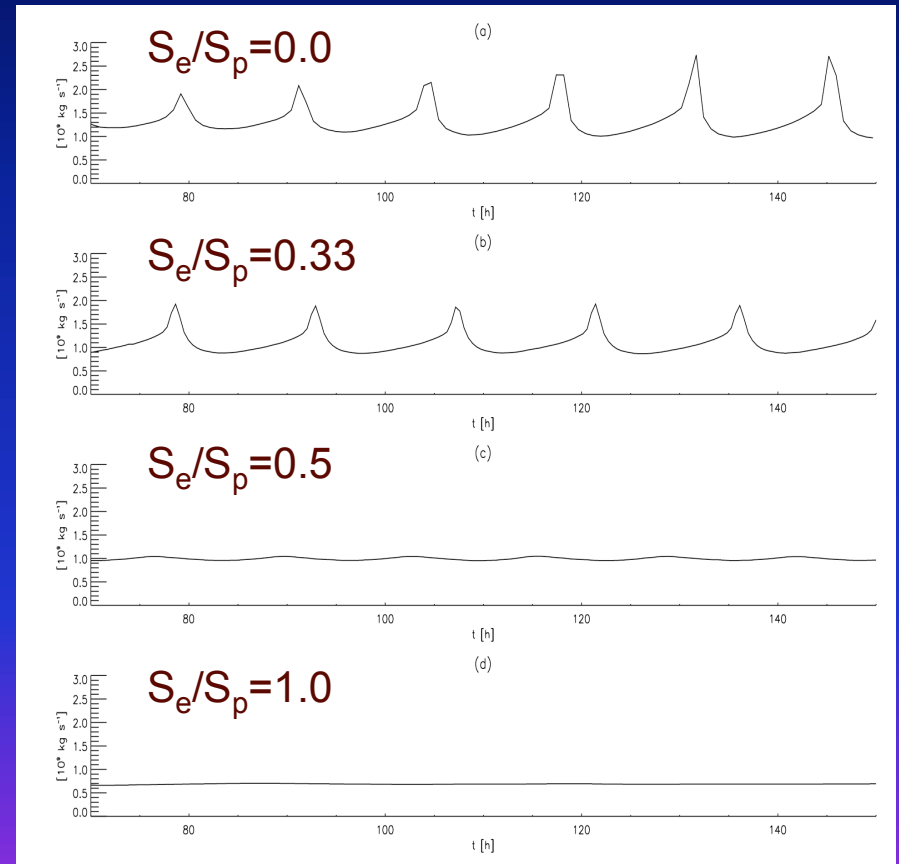
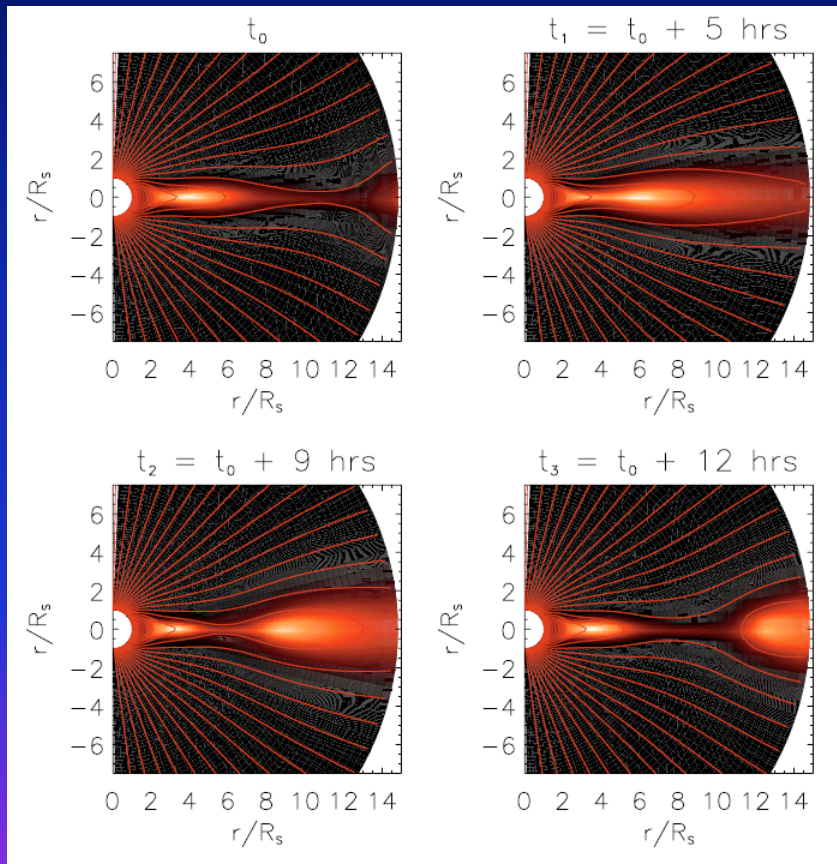


Two-Fluid Model: Streamer stability

(Endeve et al 2004)

Streamer evolution

Mass loss rate at $15R_s$



Instability occurs in the two-fluid model when the heat is deposited mostly into protons.

Polytropic MHD model

$$\frac{\partial \rho}{\partial t} + \rho \cdot (\nabla \cdot \mathbf{V}) = 0,$$

$$\rho \left[\frac{\partial \mathbf{V}}{\partial t} + (\mathbf{V} \cdot \nabla) \mathbf{V} \right] = -\nabla p - \frac{GM_S \rho}{r^2} + \frac{1}{c} \nabla \times \mathbf{B} + \mathbf{F}_v,$$

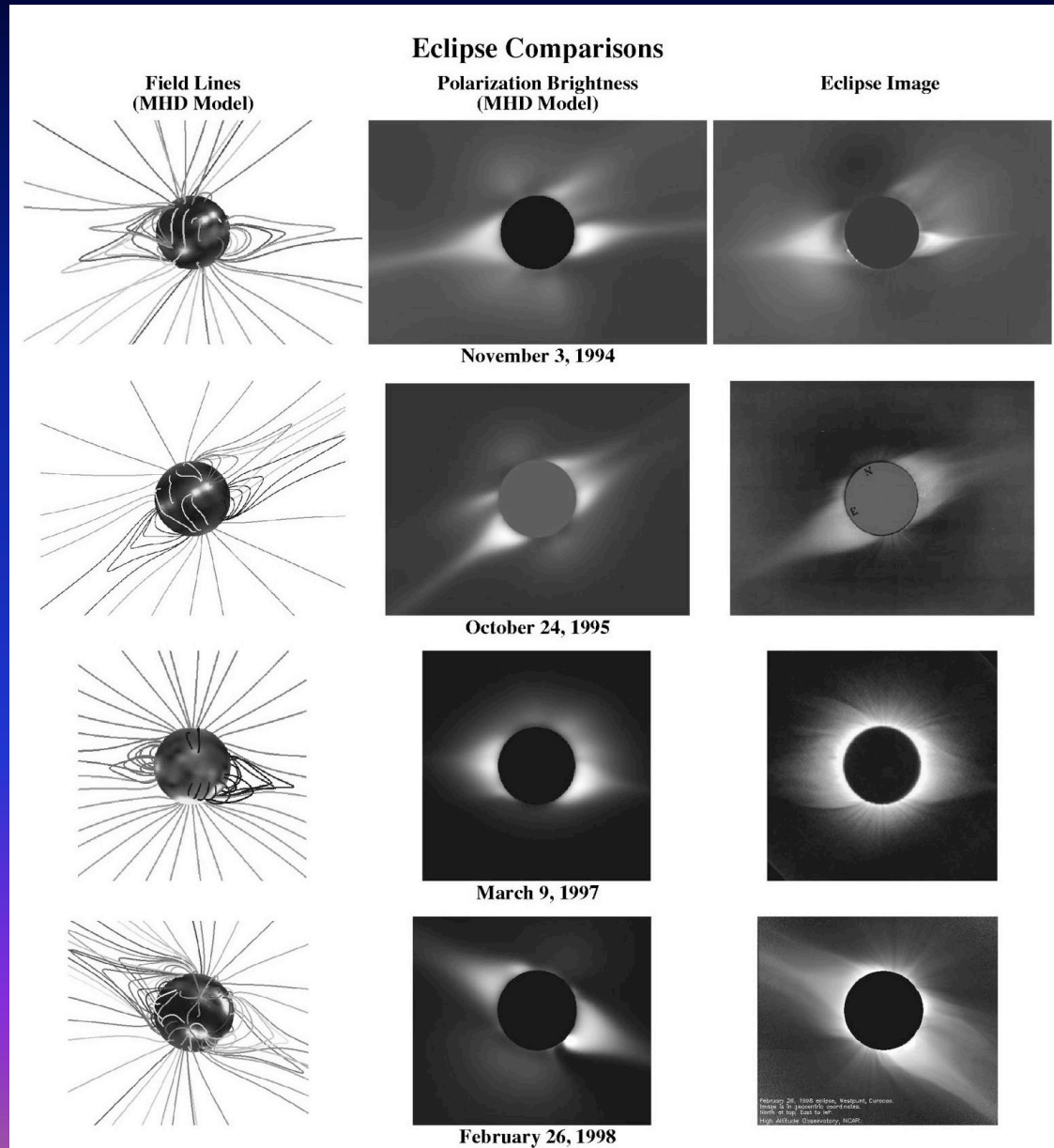
$$\frac{\partial B}{\partial t} = -c \nabla \cdot \mathbf{E}, \quad \mathbf{E} = -\frac{1}{c} \nabla \times \mathbf{B} + \mathbf{J},$$

$$\nabla \times \mathbf{B} = \frac{4\pi}{c} \mathbf{J},$$

$$\frac{\partial T}{\partial t} = (\nabla \cdot \mathbf{V}) T + \mathbf{V} \cdot \nabla T,$$

$$\gamma = 1.05$$

3D MHD polytropic model (Miki_ et al 1999)



Thermally conductive single fluid MHD model

$$\frac{\partial \rho}{\partial t} + \rho \cdot (\nabla \cdot \mathbf{V}) = 0,$$

$$\rho \left[\frac{\partial \mathbf{V}}{\partial t} + (\mathbf{V} \cdot \nabla) \mathbf{V} \right] = -\nabla p - \frac{GM_s \rho}{r^2} \hat{\mathbf{r}} + \frac{1}{c} \mathbf{J} \times \mathbf{B} + \mathbf{F}_v + \mathbf{P}_i,$$

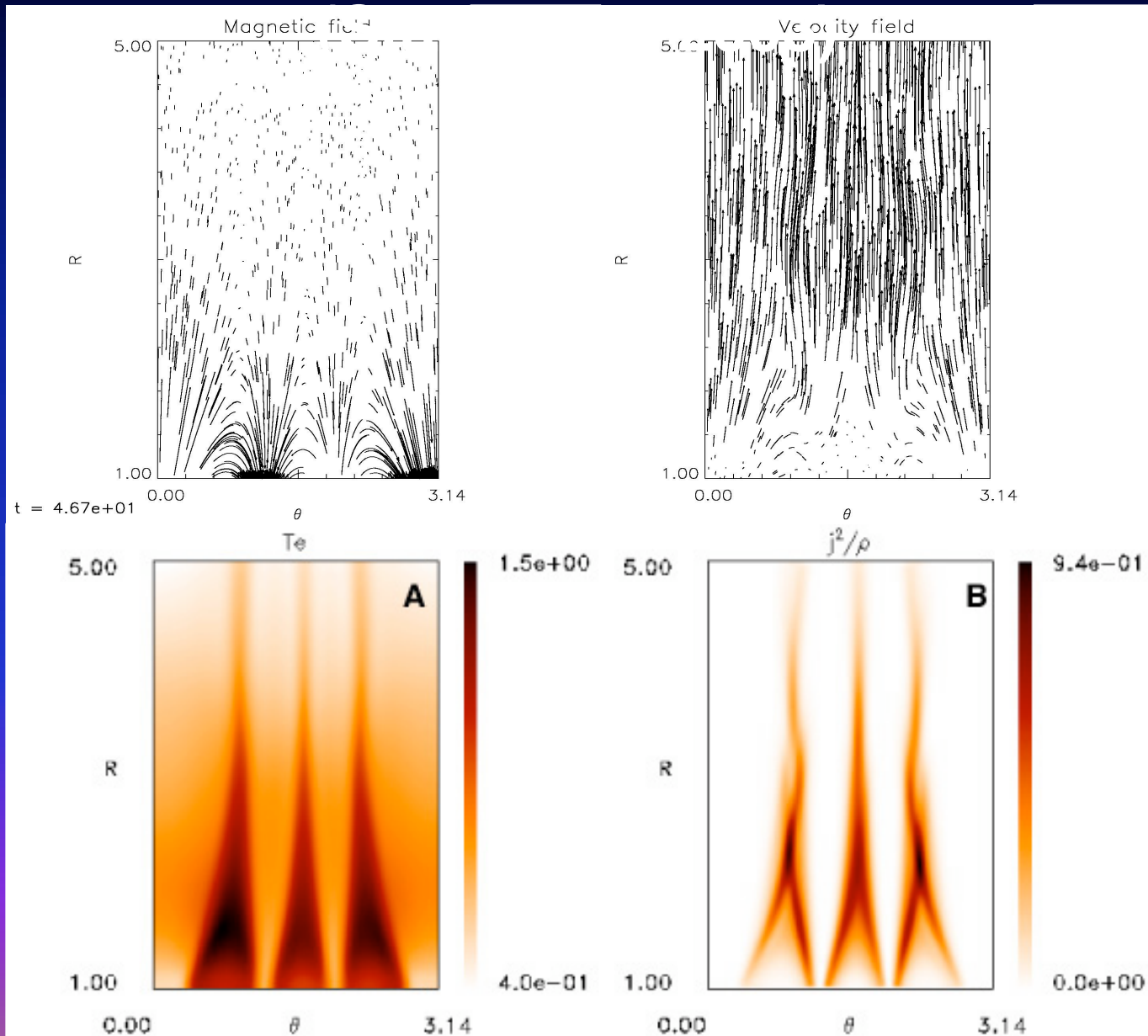
$$\frac{\partial B}{\partial t} = -c \nabla \cdot \mathbf{E}, \quad \mathbf{E} = -\frac{1}{c} \nabla \times \mathbf{B} + \mathbf{J},$$

$$\nabla \times \mathbf{B} = \frac{4\pi}{c} \mathbf{J},$$

$$\frac{\partial T}{\partial t} = -(\nabla \cdot \mathbf{V}) T + (\mathbf{V} \cdot \nabla) T + (\nabla \cdot \mathbf{H}_c) / \rho + \mathbf{H}_i,$$

$$\mathbf{H}_c = \frac{4\pi}{c} T^{5/2} \frac{\nabla T \cdot \mathbf{B}}{B^2} \hat{\mathbf{r}}, \quad \mathbf{H}_i = H_0 (r - 1) e^{r/\lambda} \hat{\mathbf{r}}, \quad P_i = P_0 f(r, \lambda)$$

Results of thermally conductive 2D MHD model

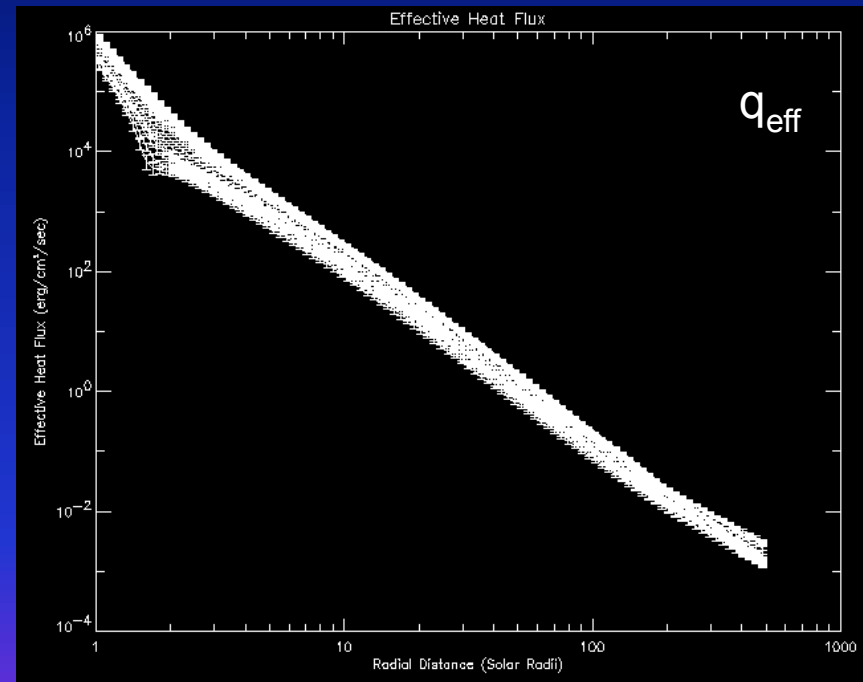
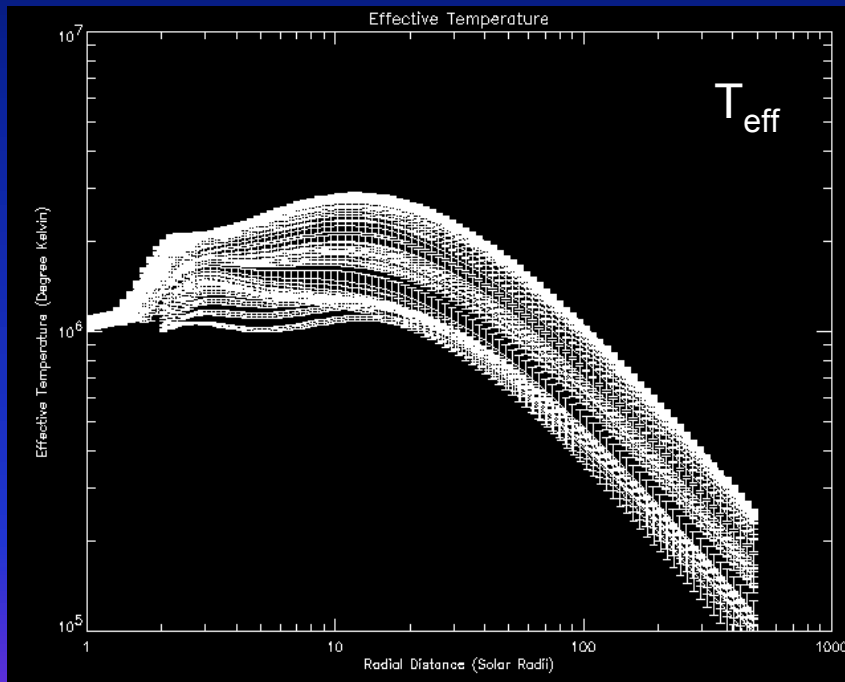


Semi-empirical model

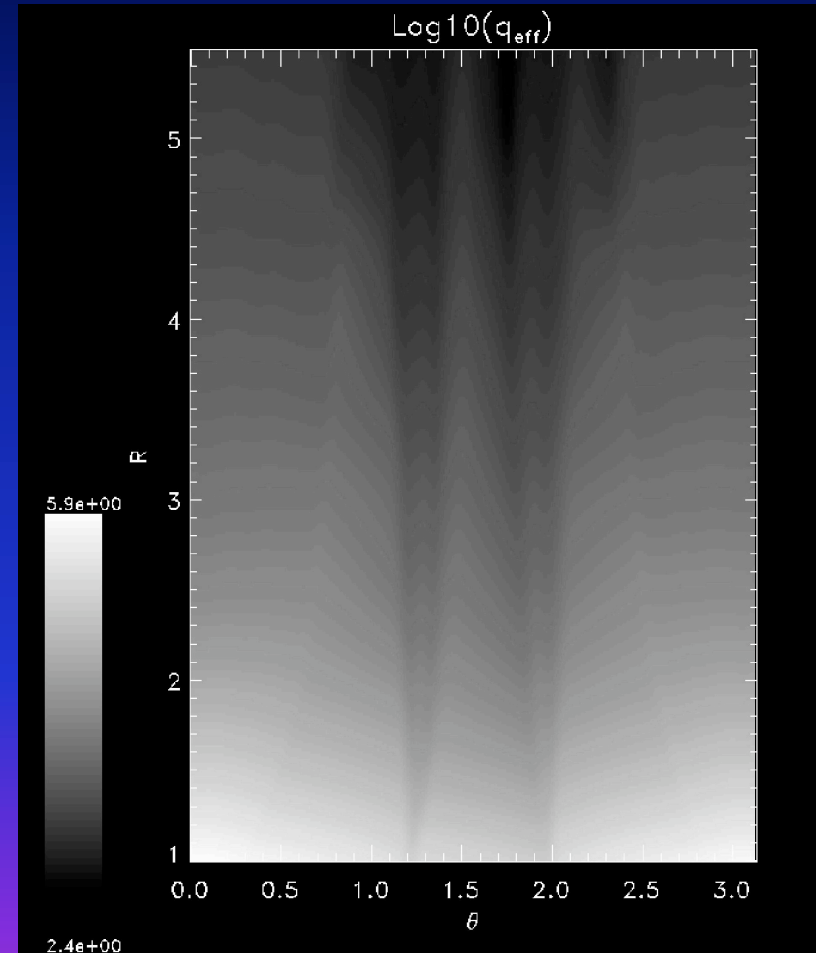
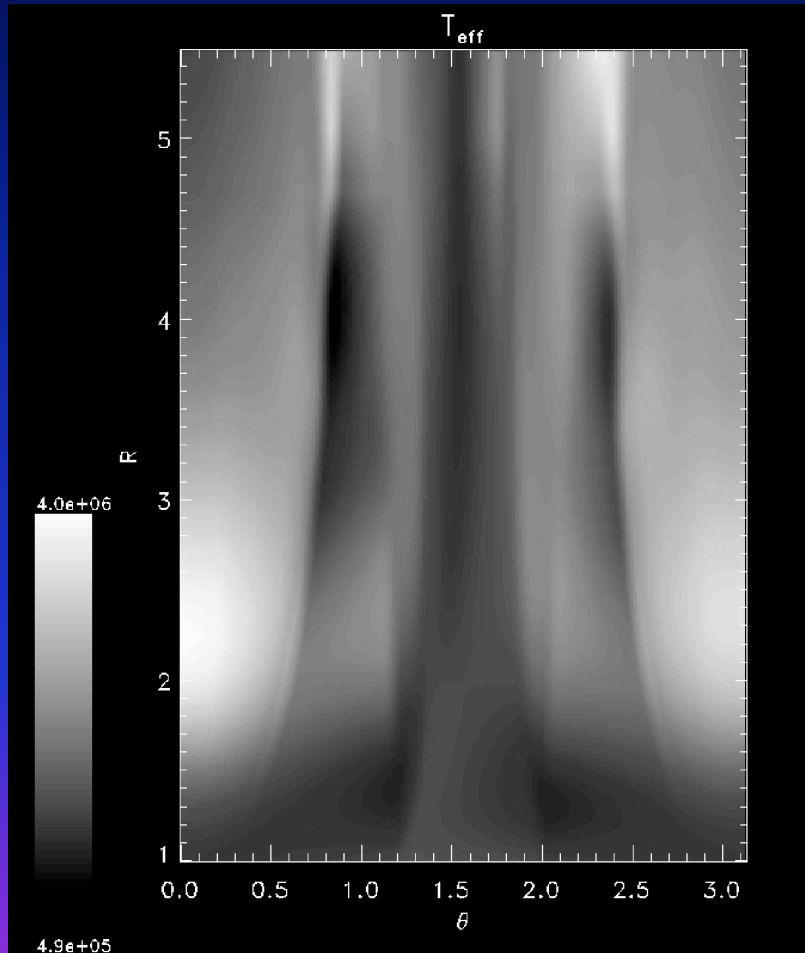
(Sittler and Guhathakurta 1999; Sittler et al 2002, 2003)

- ① The magnetic field and the SW are calculated using MHD model with photospheric boundary conditions, and a zero-order heat and momentum input.
- ② The effective heat flux and effective temperature are estimated empirically by solving energy and momentum conservation equations along open field lines using measured solar wind parameters at 1AU, and the magnetic field from #1.
- ③ The magnetic field configuration and the SW are recalculated using MHD model with updated heat flux and effective temperature.

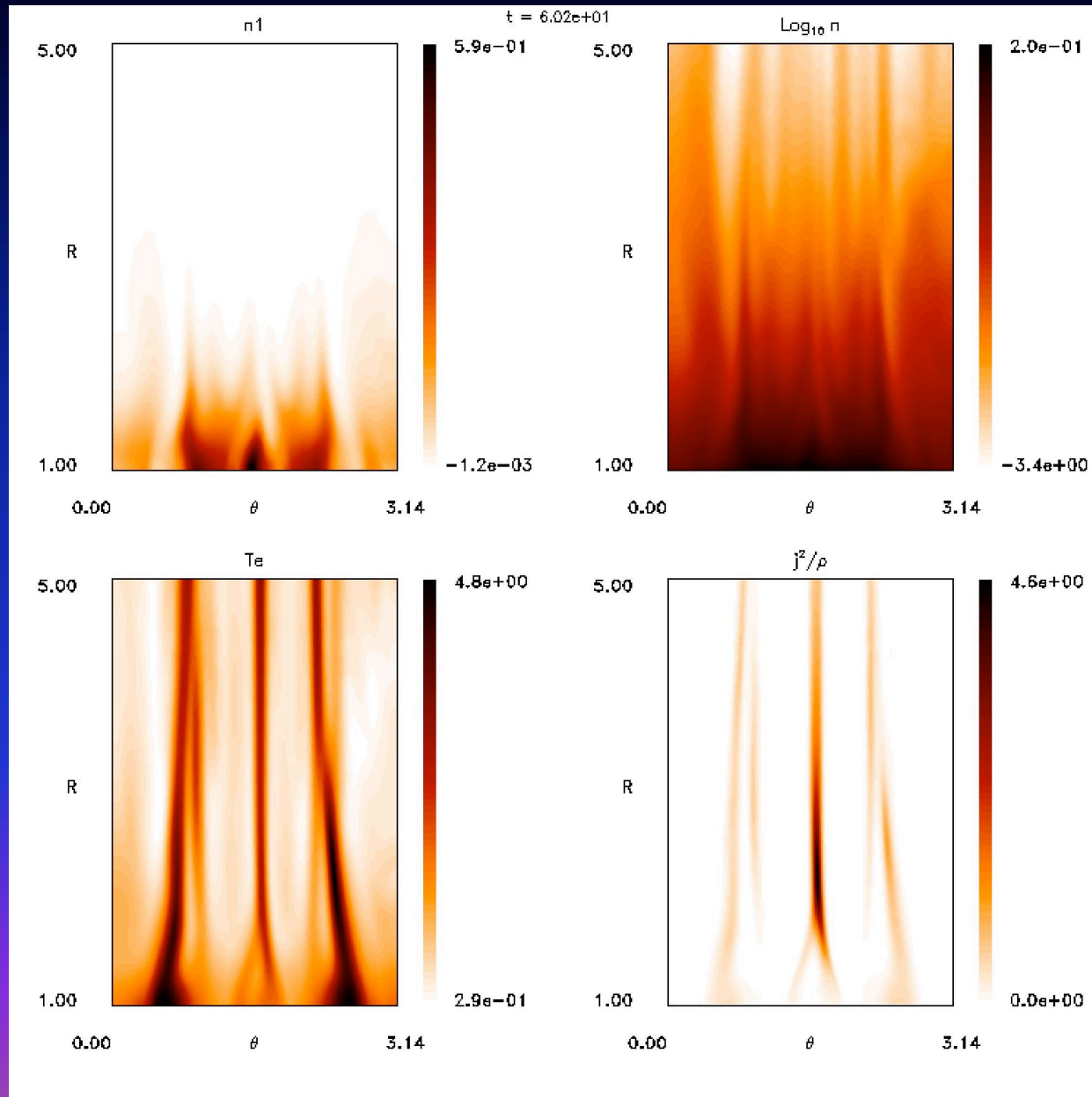
Plot of T_{eff} and q_{eff} with Error Bars for all Field Lines



Effective temperature (T_{eff}) and heat flux (q_{eff}) from Sittler et al. model



Results of Thermally Conductive MHD with q_{eff}



Conclusions

- Observations show that the physical properties of slow solar wind are strikingly different from the fast wind, and streamers can be identified as the source regions of the slow wind.
- Compositional structure of streamers in low and high FIP elements provide information on slow solar wind acceleration and origin.
- The slow solar wind in streamers has been modeled with single fluid 2D and 3D MHD codes as part of global models for decades. However, the physical mechanism that produces the slow solar wind, and the stability properties of streamers are still poorly understood.
- Recent observations of minor ion emission lines in streamers provide clues for the acceleration and heating mechanism, and require multi-fluid and kinetic modeling in order to interpret the results.
- The role of high frequency waves, low frequency waves, reconnection, and turbulence needs to be explored in streamers with multi-fluid models in order to understand how